Desalination and Water Treatment
www.deswater.com
doi: 10.1080/19443994.2014.944572

56 (2015) 536–551
October

Taylor & Francis
Taylor & Francis Group

Successful scale-up performance of a novel papaya-clay combo adsorbent: up-flow adsorption of a basic dye

Emmanuel I. Unuabonah[a,*], Adedoyin O. Adedapo[b], Cynthia O. Nnamdi[a], Adewale Adewuyi[a], Martins O. Omorogie[a], Kayode O. Adebowale[b], Bamidele I. Olu-Owolabi[b], Augustine E. Ofomaja[c], Andreas Taubert[d]

[a]*Environmental and Chemical Processes Research Laboratory, Department of Chemical Sciences, Redeemer's University, PMB 3005 Mowe, Ogun State, Nigeria, Tel. +2348053175971; emails: iyaemma@yahoo.com, unuabonahe@run.edu.ng (E.I. Unuabonah), Tel. +2348051075978; email: seentiya@yahoo.com (C.O. Nnamdi), Tel. +2348035826679; email: walexy62@yahoo.com (A. Adewuyi), Tel. +2348026827920; email: omorogiemoon@yahoo.com (M.O. Omorogie)*
[b]*Faculty of Sciences, Department of Chemistry, University of Ibadan, Ibadan, Nigeria, Tel. +2347037268274; email: pristy43@yahoo.com (A.O. Adedapo), Tel. +2348033964147; email: adebowale2003@yahoo.com (K.O. Adebowale), Tel. +2348035632025; email: iromidayobamidele@yahoo.co.uk (B.I. Olu-Owolabi)*
[c]*Faculty of Applied and Computer Science, Biosorption and Water Treatment Research Laboratory, Department of Chemistry, Vaal University of Technology, P. Bag X021, Vanderbijlpark 1900, South Africa, Tel. +27745408161; email: aus_ofomaja@yahoo.com (A.E. Ofomaja)*
[d]*Institute of Chemistry, University of Potsdam, D-14476 Potsdam, Golm, Germany, Tel. +493319775773; email: ataubert@unipotsdam.de (A. Taubert)*

Received 21 November 2013; Accepted 12 June 2014

ABSTRACT

A novel novel low-cost papaya-clay combo adsorbent, hybrid clay (HYCA), was prepared from a combination of *Carica papaya* seeds and Kaolinite clay. HYCA breakthrough adsorption capacity was 35.46 mg/g for the adsorption of methylene blue (MB) dye in a pilot-scale fixed-bed reactor. In ca. 20 min, regeneration of MB dye-loaded HYCA reached at least 90% each cycle for five regeneration cycles. However, above 40˚C, the HYCA adsorbent lost more than 50% of its adsorption capacity after five regeneration cycles. The AdDesignS^{TM} software was used to successfully predict the breakthrough curve and scale-up performance of MB dye adsorption onto the HYCA adsorbent. The pore and surface diffusion model (PSDM) described experimental data better than the constant pattern homogeneous surface diffusion model. From economic assessment using the PSDM, the AdDesignS^{TM} software predicted that 1 kg of HYCA can effectively treat 1.45 m^3 (0.29 m^3 each cycle) of water containing 1 mg/L of MB dye (with a treatment objective of 50 µg/L MB dye) in effluent solution in 9 h 35 min with run time of ca. 15 h in a day including time for five regeneration cycles It was further predicted that the presence of other organic pollutants in low concentrations reduce the breakthrough adsorption capacity of HYCA by 10%. Finally, the cost of preparing 1 kg of HYCA adsorbent was calculated to ≈$6.31 vs. ≈$31.25/kg for medium quality commercial activated carbon.

Keywords: Hybrid clay; Cationic dye; Methylene blue; Breakthrough; Adsorption; Regeneration; Pore and surface diffusion model

*Corresponding author.

1. Introduction

Dyes are broadly used as coloring agents in a variety of industries, such as textiles, cosmetics, pulp mills, leather, dye production, printing, food, and plastics [1]. Many of these organic dyestuffs are harmful to human beings and hazardous to aquatic organisms especially when wastewater containing these dyestuffs is disposed directly into water bodies without pretreatment [2]. Thus, there is a worldwide need to remove (organic) dye molecules from aqueous media on a very large scale. Among the numerous dye removal techniques available, adsorption is the preferred method and gives the best results. The main advantage over other approaches is that it can be used to remove a very broad spectrum of colorants. However, as conventional adsorbents such as activated carbon and zeolites are fairly expensive, many industries in the developing countries using dyes still practice an indiscriminate discharge of dye effluents into water bodies and thus, often severely harm the environment and the population.

Methylene blue (MB) has numerous applications, including coloring paper, temporary hair colorant, dyeing cottons, wools, and coating for paper stock. Although MB is not highly toxic, it does cause harm at elevated concentration. Acute exposure to MB can lead to increased heart rate, vomiting, shock, Heinz body formation, cyanosis, jaundice, quadriplegia, and tissue necrosis in humans [3].

The harmful effects of dye molecules and the high cost of conventional adsorbents have thus piqued interest in true low-cost adsorbents for dye removal. Low-cost materials that have been studied include, but are not limited to, acrylic acid-grafted cellulosic *Luffa cylindrical* fibers [4], sodium hydroxide-modified diatomite [5], clay–polymer composites [6], polymer–agrowaste composites [7], garlic peel [8], and solid waste-derived activated carbon [9]. However, most of these new materials have not been applied on a large scale either because some of these materials (especially agrowaste materials not well prepared) "bleed" into solutions under treatment or because the materials do not have sufficient density to even withstand a fixed-bed pilot-scale test.

Defatted *Carica papaya* seeds and kaolinite clay have also been used to remove MB from aqueous solution, although with limited success [10]. In spite of this, we have recently prepared a novel low cost but very efficient adsorbent for heavy metals called "HYCA" (hybrid clay) from a combination of kaolinite clay and *C. papaya* seeds [11], but this material has not been used for removal of organic dyes yet. The HYCA adsorbent (i) can be made from raw materials that are abundant in many developing countries, (ii) has been proven successful for heavy metal removal, (iii) does not "bleed" into solution, and (iv) has a density ($2.210\ g/cm^3$) suitable for fixed-bed pilot studies. HYCA, therefore, clearly is a candidate for the replacement of the much more expensive activated carbon or zeolite adsorbents. It is thus imperative to study its performance on a scale-up level.

This study, therefore, investigates the performance of HYCA for the removal of the cationic dye MB from aqueous solution. The influence of several process variables relevant to the adsorption process (initial dye concentration, bed height, temperature, flow rate) was considered. The regeneration of the HYCA adsorbent and the impact of some of these operational variables on the overall regeneration process were also studied. Finally, we used the AdDesignS^{TM} software to successfully predict the large-scale performance of the HYCA material.

MB dye was chosen as a model because it strongly interacts with many solids and is often used as a model compound for the adsorption of cationic organic compounds on aqueous solution.

2. Materials and methods

2.1. Materials

C. papaya seeds were taken from several open markets in Nigeria and sun dried until all the fleshy parts of the fruits were dried off the seed and subsequently stored in an airtight container. Kaolinite clay was collected from Redeemer's University, Redemption City, Mowe, Ogun State, Nigeria. After collection, stones and other heavy particles were removed from the sample. The kaolinite clay sample was further purified according to Adebowale et al. [12]. MB ($C_{16}H_{18}N_3SCl$, [7-(dimethylamino)phenothiazin-3-ylidene]-dimethylazanium chloride, C.L Basic Blue 9, 373.9 g/mol, analytical grade) and NaOH (analytical grade) were obtained from Merck Chemicals and used without further purification.

HYCA was prepared according to Unuabonah et al. [11]. Equal weights (10 g each) of purified clay and dried papaya seeds were weighed into a 500-mL beaker with 200 mL of 0.1 M NaOH and stirred. The mixture was left standing for 3 d with intermittent stirring after which it was transferred to an oven and held at 105°C until the sample was dried. Samples of the dried mixture were weighed into a crucible and calcined in a furnace at 300°C for 6 h in air. The resultant dark powdery material was washed in a Salamander fixed-bed reactor (Salamander Tubular Reactor, *The Cambridge Reactor Design*, Unit D2, Fig. 1) to

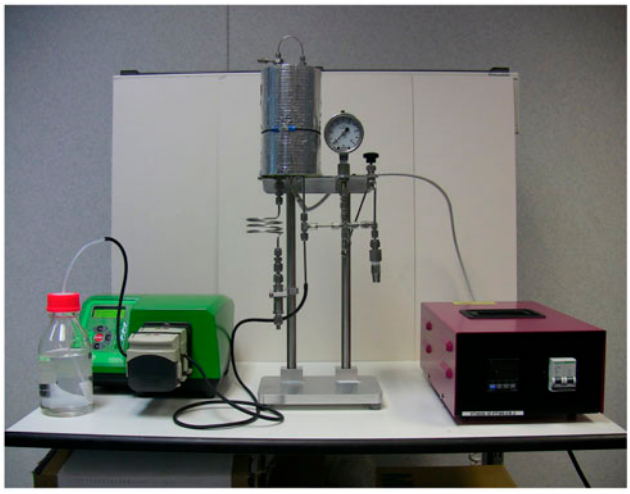

Fig. 1. Photograph of the Salamander fixed-bed reactor.

remove residual NaOH from the surface of the composite using 0.01 M of HNO_3 and subsequently deionized water. The samples were then dried in an oven at 100˚C. The dried samples were stored in an airtight container. Characterization was done as described previously [11].

2.2. Effect of operation variables on MB adsorption on HYCA

To evaluate the performance of the HYCA material, several variables were considered: (i) initial MB concentration, (ii) bed height, (iii) temperature, and (iv) flow rate. For evaluation of the initial MB concentration, a stock solution of 1,000 mg/L of MB in deionized water was used. Solutions with MB concentrations of 1, 10, and 15 mg/L were prepared from this stock solution. They were allowed to flow through 2 g (14.5 cm bed height) of HYCA adsorbent in a Salamander fixed-bed reactor at 5 mL/min by upward flow mode at 30˚C. The influence of temperature was studied by passing a 15 mg/L MB solution through the same setup (2 g, 14.5 cm bed height) and the same conditions (5 mL/min, upward flow mode) at 30, 40, and 50˚C. Similarly, the effect of bed height was investigated using three bed heights: 3.25 cm (0.5 g of HYCA), 7.25 cm (1.0 g), and 14.5 cm (2.0 g) again for the adsorption of 15 mg/L of MB solution at 5 mL/min. Finally, the effect of flow rate was studied with three flow rates: 5, 7.5, and 10 mL/min using a bed height of 14.5 cm, an MB concentration of 15 mg/L, and a reactor temperature of 30˚C.

At specific time intervals, effluent samples were taken from the fixed-bed reactor and MB dye concentrations were determined immediately via UV–vis spectroscopy (Shimadzu 1650pc UV–vis spectrophotometer).

2.3. MB dye desorption from HYCA

Two gram of HYCA was weighed into the fixed-bed reactor and a 145 mg/L MB solution was passed through the bed via upward flow mode for 4 h to ensure full loading of the adsorbent. The adsorbent bed was then washed with deionized water (pH 6.95) to remove excess MB from the HYCA surface. Subsequently, aqueous HNO_3 was pumped through the bed by upward flow. To evaluate MB desorption from HYCA, three parameters were varied: HNO_3 concentration (0.001, 0.01, and 0.1 M), flow rate (5, 10, and 15 mL/min), and temperature (30, 40, and 50˚C). To reintroduce MB onto the adsorbent in the reactor after each regeneration cycle, the adsorbent in the fixed-bed reactor was first flushed with deionized water before reloading with 145 mg/L of MB dye.

Experimental desorption results were modeled with a first-order parabolic desorption rate model:

$$F/F_{\text{initial}}(t) = f_o - f_o e^{-k_{\text{des}}t} + bt^{0.5} \quad (1)$$

where $F/F_{\text{initial}}(t)$ is the fraction of MB desorbed at time t, f_o is the fraction of MB desorbed by the fast reaction, k_{des} is the rate constant of the fast desorption (min^{-1}), and b is the rate constant of the slow MB desorption ($\text{min}^{-0.5}$). The parameters f_o, k_{des}, and b were determined by minimizing the sum of squared differences between the experimental and predicted values of the dependent variable using the quasi-Newton least square algorithm implemented in KyPlot 2.0 (KyensLab Inc., Tokyo).

2.4. Fixed-bed models

Adsorption is complex and affected by many variables. The effluent concentration from the fixed bed, rate of uptake, and the maximum bed capacity of an adsorption column are performance parameters of practical importance to the design of the adsorption process on a large scale. They are usually predicted by mathematical models [13]. Some of these models are limited in their ability to accurately predict breakthrough behavior because their mathematical solutions do not consider certain factors that influence a breakthrough curve and hence parameters obtained from such. For example, the Thomas model neglects the influence of axial dispersion during the adsorption

process and assumes that the rate-driving force for the adsorption process obeys second-order reversible reaction kinetics [14].

These models often have simple mathematical solutions yet they have been successfully used by numerous authors e.g. Thomas [15], Adams–Bohart [16], Clark [17], and Yoon–Nelson [18] model. Their practical importance stems from their ability to rapidly provide both qualitative and quantitative information describing the efficiency of an adsorbent in a fixed bed, especially in terms of its capacity and rate of uptake. These models, however, do lack the ability to predict the efficiency of the adsorbent in large adsorption systems.

More sophisticated models such as the linear driving force model, the surface diffusion model [19], the pore diffusion model [20], the diffusion flow–film particle diffusion model [21], the film pore and surface diffusion model [22,23], the pore and surface diffusion model (PSDM) [22], and the constant pattern homogeneous surface diffusion model (CPHSDM) [19] can predict adsorption capacity, uptake rate, advection/convection diffusion, axial and radial dispersions, and breakthrough curves more accurately than the simpler models. Their significant disadvantage over the simpler models is that they require extensive numerical analysis, which often makes them unpractical.

We have, in the past, successfully used the Thomas model to evaluate adsorption on the HYCA material [11]. We have, therefore, again used this model to predict the breakthrough adsorption capacity of HYCA adsorbent and the MB uptake rate. In a complementary analysis, we have used the PSDM and CPHSDM (implemented in the AdDesignS^{TM} software, CenCITT, Michigan Technological University, USA) to describe the breakthrough curve and to predict the efficiency of the HYCA adsorbent in large adsorption systems.

2.4.1. Thomas model

Thomas model is one of the most general and widely used methods in column performance theory. The model has the following form [15]:

$$\frac{C_t}{C_o} = \frac{1}{1 + \exp[k_{TH} q_o {}^{x}/_{F_m} - k_{TH} C_o t]} \quad (2)$$

or in the linearized form:

$$\ln\left(\frac{C_o}{C_t} - 1\right) = \frac{k_{TH} q_o x}{F_m} - k_{TH} C_o t \quad (3)$$

The ratio C_t/C_o is the ratio of the effluent and the influent (adsorbate) concentrations and M is the adsorbent mass (g). The kinetic coefficient, k_{TH} (mL min^{-1} mg^{-1}), and the adsorption capacity, q_o (mg/g) can be obtained from the plot of C_t/C_o against time t (min) at a given flow rate using non-linear regression. C_0 is the initial dye concentration (mg/L), x is the weight of adsorbent (g), C_t is the concentration of dye at time t (mg/L), and F_m is the flow rate of the influent solution. The parameters q_o and k_{TH} were determined by minimizing the sum of squared differences between the experimental and predicted values of the dependent variable using the quasi-Newton least square algorithm implemented in KyPlot 2.0.

2.4.2. Constant pattern homogeneous surface diffusion model

AdDesignS^{TM} software was used to model experimental data against the CPHSDM. The CPHSDM is a fixed-bed adsorption model for a single compound developed by Hand et al. [19]. It uses the following assumptions: (i) constant flow rate, (ii) plug-flow conditions exist in the bed, (iii) linear driving force which describes the local bulk-phase mass flux at the exterior surface of the adsorbent particle, (iv) surface diffusion is the predominant intraparticle mass transfer mechanism and is not a function of concentration, (v) a local adsorption equilibrium exists between the solute adsorbed on the adsorbent and the solute in the adsorbent pores, and (vi) the adsorption equilibrium is represented by the Freundlich equation.

For a favorably adsorbed compound ($1/n < 1$, where n is the Freundlich constant), the mass transfer zone increases in length as it travels through a fixed bed until it attains a constant shape (or constant pattern). The CPHSDM is based on rather simple algebra eliminating the need to solve complex differential equations that usually describe the adsorption dynamics. This results in a short calculation time. However, to obtain solutions to the CPHSDM, some restrictions are necessary: (i) the influent concentration should roughly be constant and only fluctuate by at most 30% and (ii) the fixed bed should be long enough such that there is enough time for the mass transfer wave to develop within 10% of constant pattern conditions. This is only possible if $1/n < 1$. The complete mathematics has been published by Hand et al. [19] and is also summarized in Appendix B of the AdDesignS^{TM} manual. Input data used for the AdDesignS^{TM} software are shown in Table 1.

2.4.3. Pore and surface diffusion model

The PSDM is a dynamic fixed-bed model that incorporates the following assumptions: (i) constant flow rate, (ii) plug-flow conditions exist in the bed, (iii) a linear driving force describes the local bulk-phase mass flux at the exterior surface of the adsorbent particle, (iv) a local adsorption equilibrium exists between the solute adsorbed on the adsorbent and the solute in the intra-aggregate stagnant fluid, (v) intraparticle mass flux is described by surface and pore diffusion, (vi) the adsorption equilibrium of individual compounds can be represented by the Freundlich equation, (vii) ideal absorbed solution theory describes the competition between the compounds, and (viii) there are no interactions between adsorbing compounds during the diffusion process.

The various partial differential equations for PSDM have been solved by numerical, orthogonal collocation, and backward differential methods [24–26], while Crittenden et al. [22] and Friedman [27] have presented the derivation of the equations and the computer algorithms that were used to solve the model equations. The PSDM model equations are summarized in Appendix C of the AdDesignS^{TM} manual.

Adsorption calculations using this model require: (i) equilibrium and kinetic parameters and (ii) physical properties of the adsorbing compound(s) and the adsorbent. These parameters are implemented in the AdDesignS^{TM} databases, which also contain parameter estimation modules. PSDM requires much more calculation time than CPHSDM but it provides breakthrough curves for each compound. Input data used for the AdDesignS™ software are shown in Table 1.

3. Results and discussion

3.1. Thomas model analysis

3.1.1. Effect of initial dye concentration

The effect of initial MB dye concentration on the adsorption of MB dye onto HYCA is shown in Fig. 2 and Table 2. Fitting the experimental data with the Thomas model shows that the breakthrough adsorption capacity (q_e) increases with increasing initial MB

Table 1
Input data for PSDM and CPHSDM modeling using AdDesignS^{TM} software

Input data for CPHSD Model	
Chemical	
Molecular weight of MB dye	373.90 g/mol
Initial concentration	Variable (1, 10 and 15 mg/L)
Bed data	
Bed length	3.625×10^{-02} m
Bed diameter	6.000×10^{-03} m
Weight of HYCA	Variable (0.5, 1.0 and 2.0 g)
Inlet flow rate	Variable (5.0, 7.5 and 15 mL/min)
Temperature	Variable (30, 40 and 50°C)
Water density	Variable (30°C = 0.9957 g/cm^3; 40°C = 0.9922 g/cm^3; 50°C = 0.9880 g/cm^3)
Water viscosity	8.15×10^{-03} g/cm s
Input data for PSD model	
Chemical	
Molecular weight of MB dye	373.90 g/mol
Initial concentration	Variable (1, 10 and 15 mg/L)
Bed data	
Bed length	3.625×10^{-02} m
Bed diameter	6.000×10^{-03} m
Weight of HYCA	Variable (0.5, 1.0 and 2.0 g)
Inlet flow rate	Variable (5.0, 7.5 and 15 mL/min)
Temperature	Variable (30, 40 and 50°C)
Water density	Variable (30°C = 0.9957 g/cm^3; 40°C = 0.9922 g/cm^3; 50°C = 0.9880 g/cm^3)
Adsorbent properties	
Name	HYCA
Apparent density	2.210 g/cm^3
Particle radius	0.030000 cm
Porosity	1.000

concentration and with increasing bed height and flow rate. At the same time, the overall rate of adsorption decreases. More favorable and steep breakthrough curves were obtained at highest influent dye concentration of 15 mg/L. The reason for better column performance and steep breakthrough curves at higher influent MB dye concentration is the increasing driving force of the dye molecules toward the active sites on the adsorbent and rapid utilization of adsorption sites in HYCA adsorbent [28,29]. Compared with the adsorption capacities of rice husk, olive pomace, and natural zeolite (4.16, 7.12, and 3.51 mg/g, respectively) [30–32], the HYCA adsorbent shows a better adsorption capacity (35.45 mg/g) even though the initial concentration of MB dye and flow rate used in the case of the other adsorbents were significantly higher than those for HYCA adsorbent.

3.1.2. Effect of bed height

The effect of bed height on the adsorption of MB dye onto HYCA adsorbent is shown in Fig. 3 and Table 2. Data analysis with the Thomas model suggests that increased bed heights increase the breakthrough adsorption capacity (Table 2). Increasing breakthrough adsorption capacity with increasing bed height leads to a corresponding decrease in the rate of MB adsorption on the column. The reason is the decreased diffusivity of the dye through the column due to axial dispersion during mass transfer. This implies that the solute, MB dye, spends more time in the column interacting with the adsorbent due to availability of more adsorption sites on the adsorbent (HYCA). This obviously accounts for the decrease in the overall rate of adsorption of the MB dye by the adsorbent [33].

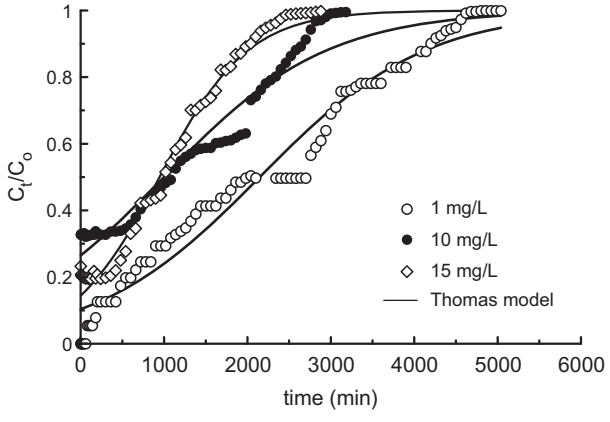

Fig. 2. Thomas model plot for the adsorption of MB dye onto HYCA adsorbent at various initial dye concentrations.

Table 2
Parameters of Thomas model using non-linear regression analysis at various operating variables

	k_{TH}	q_o	r^2	% Error
Effect of initial dye concentration				
1 mg/L	1.00	5.37	0.9667	0.35
10 mg/L	0.10	24.95	0.9475	0.29
15 mg/L	0.13	35.46	0.9890	0.11
Effect of bed height				
3.25 cm	0.42	22.53	0.9350	0.55
7.25 cm	0.15	35.03	0.9734	0.21
14.5 cm	0.13	35.46	0.9890	0.11
Effect of temperature				
30°C	0.13	35.46	0.9890	0.11
40°C	0.12	37.83	0.9868	0.13
50°C	0.10	41.20	0.9753	0.21
Effect of flow rate				
5 mL/min	0.13	35.46	0.9890	0.11
7.5 mL/min	0.17	34.18	0.9787	0.21
10 mL/min	0.34	26.15	0.9949	0.06

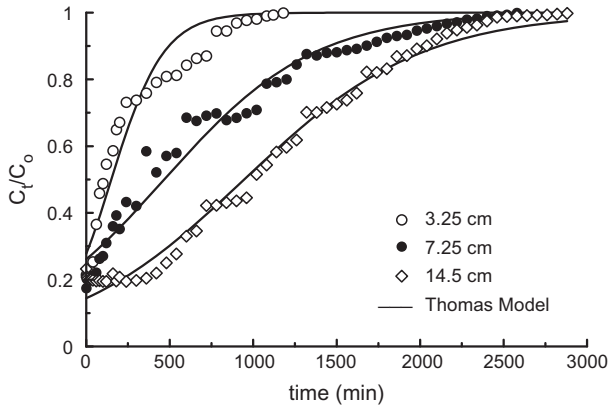

Fig. 3. Thomas model plot for the adsorption of MB dye onto HYCA adsorbent at various bed heights.

3.1.3. Effect of temperature

The effect of temperature on MB adsorption on HYCA is shown in Fig. 4 and Table 2. Increasing temperature favors the adsorption of MB on HYCA as seen from the corresponding increase in breakthrough adsorption capacity shown by the Thomas model (Table 2). This may suggest that MB adsorption on HYCA is endothermic. Increasing temperature may also enhance the diffusivity of MB in the fixed bed and hence, provide a higher frequency of favorable contacts between MB and HYCA leading to an overall improved adsorption.

3.1.4. Effect of flow rate

The breakthrough adsorption capacities at flow rates of 5, 7.5, and 10 mL min^{-1} are ca. 36, 34, and 26 mg g^{-1}, respectively (Table 2). The decrease in breakthrough adsorption capacity with increasing flow rate is likely due to the reduced contact time between solute and adsorbent, possibly leading to a non-equilibrium situation which does not provide enough residence time in the column for complete adsorption of the dye at higher flow rates. Similar results were obtained by Singh and Pant [34–36]. Ghorai and Pant [36] suggested that increasing flow rates in a fixed-bed system could lead loss of intraparticle film and thus increase the rate of adsorption of the solute molecule. However, at lower flow rates, external mass transfer controls the adsorption process which is ideal for intraparticle diffusion systems [37]. Thus, the dye molecules have more time to diffuse into the HYCA adsorbent particles and resulting in better breakthrough adsorption capacity (Fig. 5).

3.2. Prediction of adsorbent efficiency

Several mass transfer phenomena are involved in fixed-bed adsorption kinetics: (i) axial dispersion, (ii) external diffusion, (iii) adsorption at the fluid–particle interface, and (iv) intraparticle diffusion. For fixed-bed systems with a non-linear adsorption isotherm, it is difficult to obtain an exact analytical solution for the breakthrough curve at the exit of the adsorption bed. Thus, the design and modeling of the fixed-bed adsorption kinetics, especially in case of systems with non-linear adsorption isotherms, require extensive numerical analyses using mathematical models. The AdDesignS^{TM} software [19] is a versatile platform providing the necessary models and also contains databases and estimation methods for obtaining model parameters.

In the current study, the software was used to predict and analyze adsorption isotherms and breakthrough curves of HYCA under different conditions. Two models were used: the CPHSDM and the PSDM models (Chapters 2.4.2 and 2.4.3). Overall, the PSDM model (Fig. 6) provides a better fit to the experimental data than the CPHSDM model (Fig. 7). The results from the PSDM model are therefore used in discussions in the remaining portions of this article.

Table 3 summarizes the results from the PDSM model analysis. The PSDM model predicts that the volume of MB dye solution (m^3) that will be removed per mass unit (kg) of HYCA adsorbent (volume treated by mass, VTM) at 95% breakthrough will increase with increasing bed height, bed temperature, and flow rate but will decrease with increasing initial solute concentration.

Increasing the initial dye concentration and flow rate will decrease the breakthrough time while increasing the bed height will increase breakthrough time. Increasing temperatures tend to extend the breakthrough time because there is an increase in volume of adsorbate solution being treated by mass (VTM) of the adsorbent.

Table 3 also shows that an increase in the initial dye concentration and flow rate increases the surface diffusion coefficient (D_s) of MB. This is due to a concentration gradient which is more significant at higher flow rates.

Contrary to the effect of dye concentration and the flow rate, an increase in bed height reduces the surface diffusion coefficient, although this effect is not strong. This decrease in surface diffusion coefficient is

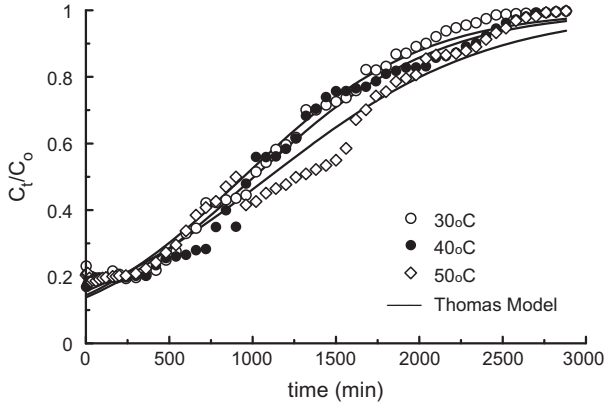

Fig. 4. Thomas model plot for the adsorption of MB dye onto HYCA adsorbent at fixed-bed temperature.

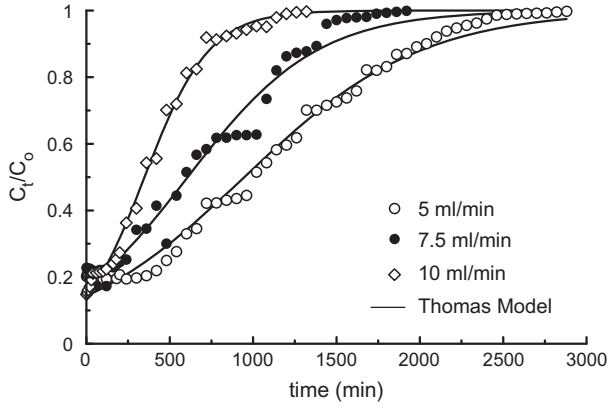

Fig. 5. Thomas model plot for the adsorption of MB dye onto HYCA adsorbent at various flow rate.

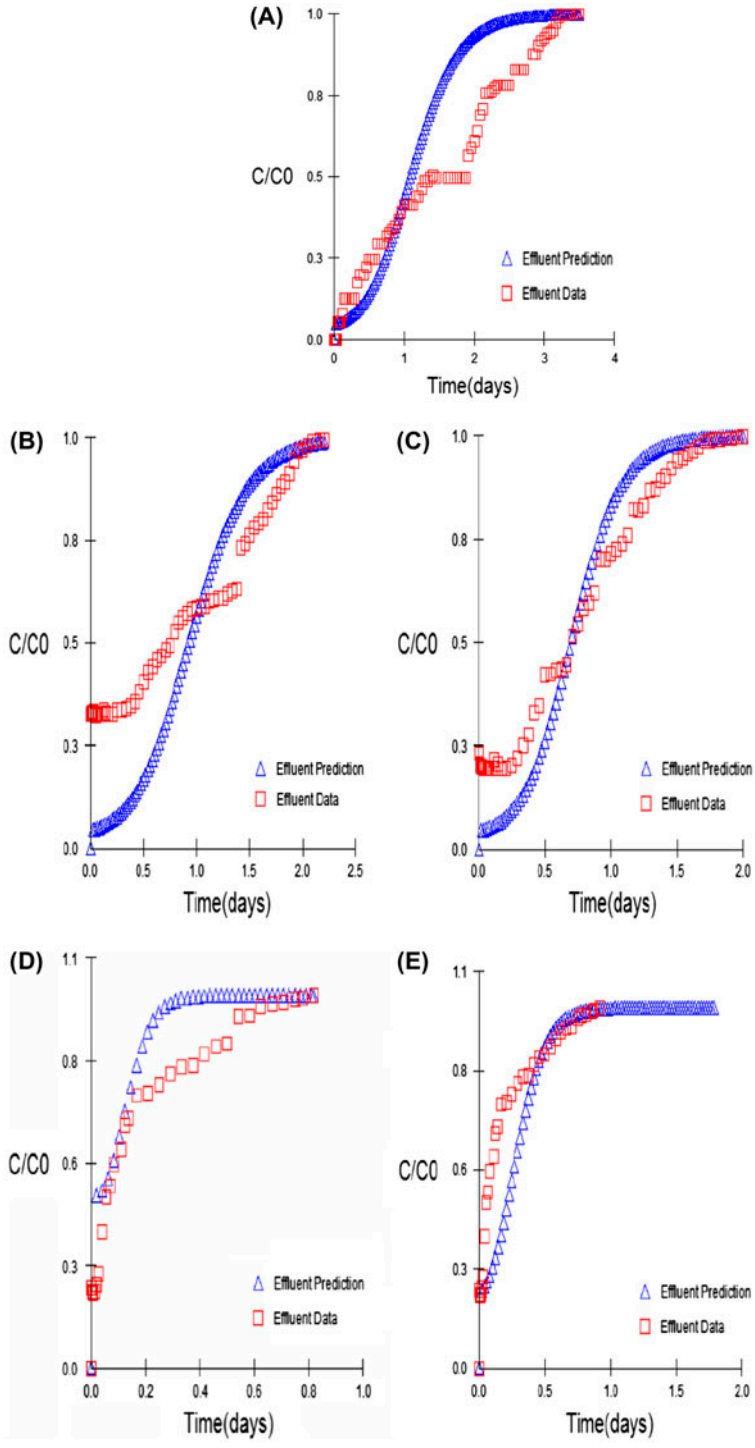

Fig. 6. PSDM plot of the adsorption of (A) 1 mg/L MB dye onto 2 g (14.5 cm) of HYCA adsorbent (Flow rate = 5 mL/min; temperature = 30˚C) (B) 10 mg/L MB dye onto 2 g (14.5 cm) of HYCA adsorbent (Flow rate = 5 mL/min; temperature = 30˚C) (C) 15 mg/L MB dye onto 2 g (14.5 cm) of HYCA adsorbent (Flow rate = 5 mL/min; temperature = 30˚C) (D) 15 mg/L MB dye onto *0.5 g (3.5 cm)* of HYCA adsorbent (Flow rate = 5 mL/min; temperature = 30˚C) (E) 15 mg/L MB dye onto *1.0 g (7.25 cm)* of HYCA adsorbent (Flow rate = 5 mL/min; temperature = 30˚C) (F) 15 mg/L MB dye onto *2.0 g* (14.5 cm) of HYCA adsorbent (Flow rate = 5 mL/min; *temperature* = 40˚C) (G) 15 mg/L MB dye onto 2 g (14.5 cm) of HYCA adsorbent (Flow rate = 5 mL/min; *temperature* = 50˚C) (H) 15 mg/L MB dye onto 2 g (14.5 cm) of HYCA adsorbent (Flow rate = 7.5 mL/min; temperature = 30˚C) (I) 15 mg/L MB dye onto 2 g (14.5 cm) of HYCA adsorbent (Flow rate = 10 mL/min; temperature = 30˚C).

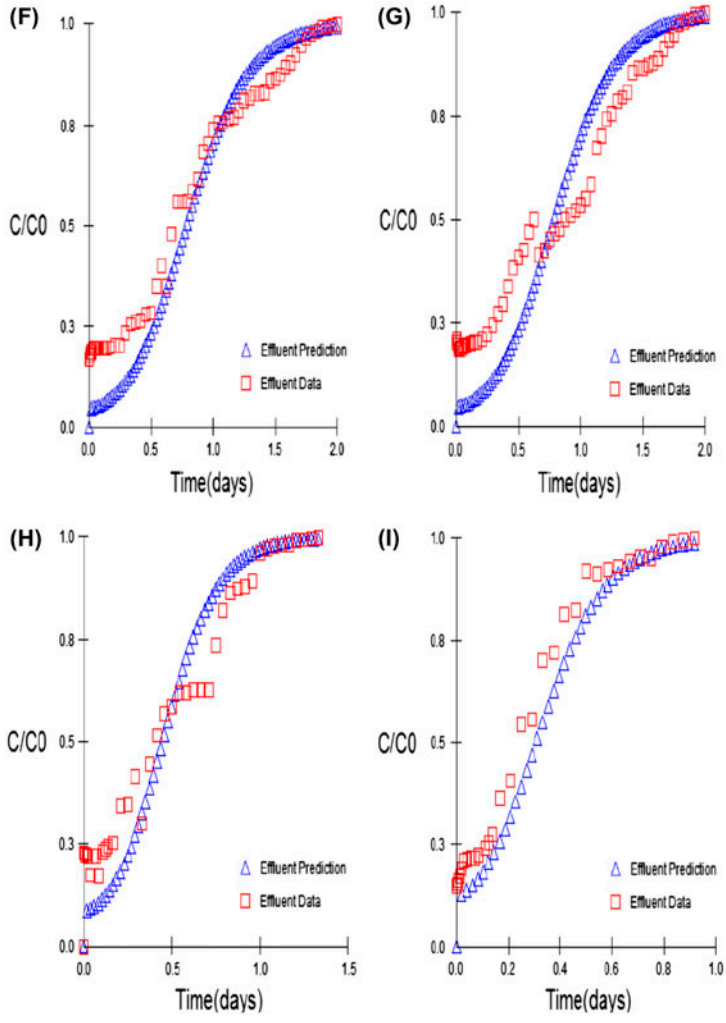

Fig. 6. (*Continued*).

as a result of an increased residence time of the dye molecule as it goes through an increasing length of adsorbent bed with increasing adsorption sites (HYCA adsorbent) and reduced mobility of the dye molecule in the case of increasing temperature.

As the VTM increases with increasing flow rate, the PSDM predicts an increase in film transfer coefficient, k_f, with increasing flow rate only. Other process variables (change in initial concentration, bed height, and temperature) do not show any influence on k_f (Table 3).

The Biot number calculated from the PSDM is 1.56 for all initial concentrations, bed heights, and temperatures used in the experiments but increases slightly with increasing flow rate to 1.85 for 7.5 mL/min and 2.10 for 10 mL/min. These low Biot numbers ($0.5 < Bi < 30$) suggest that both liquid-phase and solid-phase mass transfer rates control the adsorption of MB dye on HYCA adsorbent [19].

3.3. Regeneration study

HYCA adsorbent regeneration is crucial to ensure continuous and economic operation of the adsorbent. The key requirement is the removal of the adsorbed dye from the adsorbent in the fixed bed with the smallest possible volume of an eluting solution. Regeneration should be effective without reducing the efficiency of the adsorbent. This enables the reuse of the recycled adsorbent over multiple adsorption and desorption cycles. Fig. 8 shows the desorption plots and Tables 4–6 show the corresponding kinetic data for MB desorption from HYCA extracted from these data.

Table 3
Data from PSDM prediction of experimental data using the AdDesignS™ software at various operating variables

	k_f (cm/s)	D_s (cm^2/s)	BT (days)	VTM (m^3/kg)
Effect of initial dye concentration				
1 mg/L	0.00286	6.21×10^{-9}	2.11	7.60
10 mg/L	0.00286	7.33×10^{-9}	1.76	6.32
15 mg/L	0.00286	9.87×10^{-9}	1.26	4.55
Effect of bed height				
3.25 cm	0.00286	2.17×10^{-8}	0.25	3.54
7.25 cm	0.00286	1.39×10^{-8}	0.60	4.34
14.5 cm	0.00286	9.87×10^{-9}	1.26	4.55
Effect of temperature				
30°C	0.00286	9.87×10^{-9}	1.26	4.55
40°C	0.00286	8.62×10^{-9}	1.53	5.52
50°C	0.00286	8.62×10^{-9}	1.53	5.52
Effect of flow rate				
5 mL/min	0.00286	9.87×10^{-9}	1.26	4.55
7.5 mL/min	0.00339	1.01×10^{-8}	0.92	4.96
10 mL/min	0.00384	1.08×10^{-8}	0.71	5.08

Notes: BT = breakthrough time; VTM = volume treated per mass; k_f = film transfer coefficient; D_s = surface diffusion coefficient.

Table 4 shows that changes in the concentration of the regeneration reagent, HNO_3, from 0.001 to 0.1 M at a flow rate of 5 mL/min does not significantly change the fraction of MB dye desorbed and the rate of desorption. This observation particularly applies to HNO_3 concentrations between 0.01 and 0.1 M, where the desorption efficiency ($f_o \times 100$) is approximately 90% throughout five consecutive regeneration cycles.

However, with a flow rate change from 5 to 10 mL/min and a reagent regeneration concentration of 0.01 M (HNO_3), there was no significant increase in the fraction of MB dye desorbed and the rate of desorption (Table 5). At 15 mL/min, the desorption efficiency increased slightly to ≈94%.

Table 6 shows that temperature changes from 30 to 50°C (at a constant flow rate of 15 mL/min) lead to a decrease in both the fraction of desorbed MB dye and the rate of desorption. The fraction of desorbed MB dye is very low at ca. 0.36 (36%). This is expected since the adsorption data (Section 3.1.3) results suggest that the adsorption of MB dye on HYCA is likely endothermic.

Plots for desorption of MB from HYCA are shown in Fig. 8. Overall, these data show that even after the fifth regeneration cycle, HYCA adsorbent retains its original MB adsorption efficiency unless the temperature of the adsorption system is raised to 50°C and perhaps beyond.

3.4. Economic assessment

The cost of preparing 1 kg of HYCA was calculated to ≈$6.31 (Table 7). This is dramatically cheaper than medium quality activated carbon, which currently costs ≈$31.25/kg [38]. The cost of HYCA regeneration with 0.01 M HNO_3 was calculated to be ≈$0.5/m^3. The volume of HNO_3 regenerating reagent required for regeneration of 2 g of HYCA adsorbent is ca. 300 mL at 5 mL/min since at 60 min (300 mL × 5 mL/min = 60 min of total regeneration time) and with this procedure well over 90% of MB is desorbed from fully

Table 4
Kinetic parameters of first-order parabolic desorption rate model effect of reagent concentration on regeneration of MB dye-loaded HYCA adsorbent

	f_o	k_{des}	b	r^2	% Error
0.001 M HNO_3					
1st recycle	0.85	1.32	0.0071	0.9745	0.15
2nd recycle	0.86	1.14	0.0061	0.9546	0.25
3rd recycle	0.85	1.14	0.0064	0.9591	0.24
4th recycle	0.91	1.51	0.0044	0.9838	0.09
5th recycle	0.89	1.76	0.0046	0.9846	0.08
0.01 M HNO_3					
1st recycle	0.86	1.31	0.0079	0.9711	0.20
2nd recycle	0.88	1.36	0.0059	0.9588	0.24
3rd recycle	0.89	1.46	0.0045	0.9701	0.15
4th recycle	0.89	1.52	0.0046	0.9693	0.15
5th recycle	0.87	1.61	0.0056	0.9629	0.19
0.1 M HNO_3					
1st recycle	0.83	1.22	0.0082	0.9617	0.24
2nd recycle	0.87	1.43	0.0057	0.9724	0.15
3rd recycle	0.89	1.58	0.0046	0.9841	0.08
4th recycle	0.90	1.55	0.0046	0.9810	0.10
5th recycle	0.90	1.64	0.0038	0.9846	0.07

Table 5
Kinetic parameters of first-order parabolic desorption rate model effect of change in flow rate on regeneration of MB dye-loaded HYCA adsorbent

	f_o	k_{des}	b	r^2	% Error
5 mL/min					
1st recycle	0.86	1.31	0.0079	0.9711	0.20
2nd recycle	0.88	1.36	0.0059	0.9588	0.24
3rd recycle	0.89	1.46	0.0045	0.9701	0.15
4th recycle	0.89	1.52	0.0046	0.9693	0.15
5th recycle	0.87	1.61	0.0056	0.9629	0.19
10 mL/min					
1st recycle	0.86	1.75	0.0054	0.9696	0.14
2nd recycle	0.85	1.79	0.0059	0.9601	0.18
3rd recycle	0.87	1.79	0.0043	0.9663	0.12
4th recycle	0.88	1.72	0.0042	0.9740	0.10
5th recycle	0.86	1.81	0.0050	0.9668	0.14
15 mL/min					
1st recycle	0.93	1.67	0.0030	0.9039	0.04
2nd recycle	0.94	2.13	0.0022	0.9876	0.05
3rd recycle	0.94	2.22	0.0025	0.9865	0.06
4th recycle	0.94	2.28	0.0024	0.9878	0.05
5th recycle	0.94	2.38	0.0029	0.9897	0.05

Table 6
Kinetic parameters of first-order parabolic desorption rate model effect of change in temperature on regeneration of MB dye-loaded HYCA adsorbent

	f_o	k_{des}	b	r^2	% Error
30 °C					
1st recycle	0.93	1.67	0.0030	0.9039	0.04
2nd recycle	0.94	2.13	0.0022	0.9876	0.05
3rd recycle	0.94	2.22	0.0025	0.9865	0.06
4th recycle	0.94	2.28	0.0024	0.9878	0.05
5th recycle	0.94	2.38	0.0029	0.9897	0.05
40 °C					
1st recycle	0.92	0.75	0.0035	0.9773	0.0014
2nd recycle	0.91	1.01	0.0041	0.9779	0.0012
3rd recycle	0.90	1.15	0.0045	0.9547	0.0024
4th recycle	0.90	1.11	0.0048	0.9964	0.0019
5th recycle	0.89	1.13	0.0047	0.9568	0.0023
50 °C					
1st recycle	0.91	0.61	0.0038	0.9772	0.0014
2nd recycle	0.94	0.19	0.0020	0.9899	0.0008
3rd recycle	0.48	0.59	0.0136	0.9863	0.0007
4th recycle	0.50	0.46	0.0115	0.9813	0.0009
5th recycle	0.36	0.78	0.0139	0.9805	0.0008

loaded HYCA adsorbent. The choice of 5 mL/min over 15 mL/min (which gave slightly better desorption results, Table 7) is based on the principle of achieving desorption with small volumes of regenerating reagent which is cost effective. Overall, it thus takes approximately 65 min to fully regenerate the fixed-bed reactor containing 2 g of MB-loaded HYCA (60 min for regeneration with 0.01 M HNO_3 and 5 min for flushing the reactor with deionized water to remove traces of acid).

The PSDM was used for modeling experimental data with the following input conditions: K (Freundlich parameter) = 4.00(mg/g)(L/mg)$^{1/n}$; $1/n = 0.420$; weight of adsorbent = 2 g; flow rate = 5 mL/min; temperature = 30 °C; total run time = 5,040 min; time step = 30 min; pressure = 1 atm to predict the efficiency of HYCA adsorbent (given the poor fit of CPHSDM to experimental data as shown in Fig. 7 in a large adsorber system for treatment of MB dye in aqueous solution).

Let us assume that the treatment objective is to keep the concentration of MB dye in aqueous solution at ≤ 50 μg/L (5% breakthrough). It is predicted, for example, using 2 g of HYCA adsorbent at 30 °C and a flow rate of 5 mL/min that to reduce 1 mg/L of MB dye in aqueous solution to 50 μg/L (5% breakthrough) in a fixed-bed reactor containing 1 kg HYCA adsorbent will require a breakthrough time of ca. 115 min and produce a breakthrough volume of 290 L (data not shown). Since HYCA has at least five life cycles, 1 kg of HYCA can effectively be used to treat 1.45 m^3 (0.29 m^3 each cycle) of water containing 1 mg/L of MB with a treatment objective of 50 μg/L MB dye effluent solution in 9 h 35 min with a possible run time of ca. 15 h in a day which includes five regeneration cycles of 65 min each cycle.

Table 7
Cost estimation for preparation of 1 kg of HYCA adsorbent

	Duration (h)	Amount (L)	Unit cost (USD)	Power rating (kWh)	Price (USD)
Drying oven	6	–	0.085	0.76	0.39
Activation in oven	6	–	0.15	1.5	1.35
0.1 M NaOH cost	–	5 L	0.8	–	4.00
Net cost	–	–	–	–	5.74
Overhead cost (10% of net cost)	–	–	–	–	0.57
Total cost	–	–	–	–	6.31

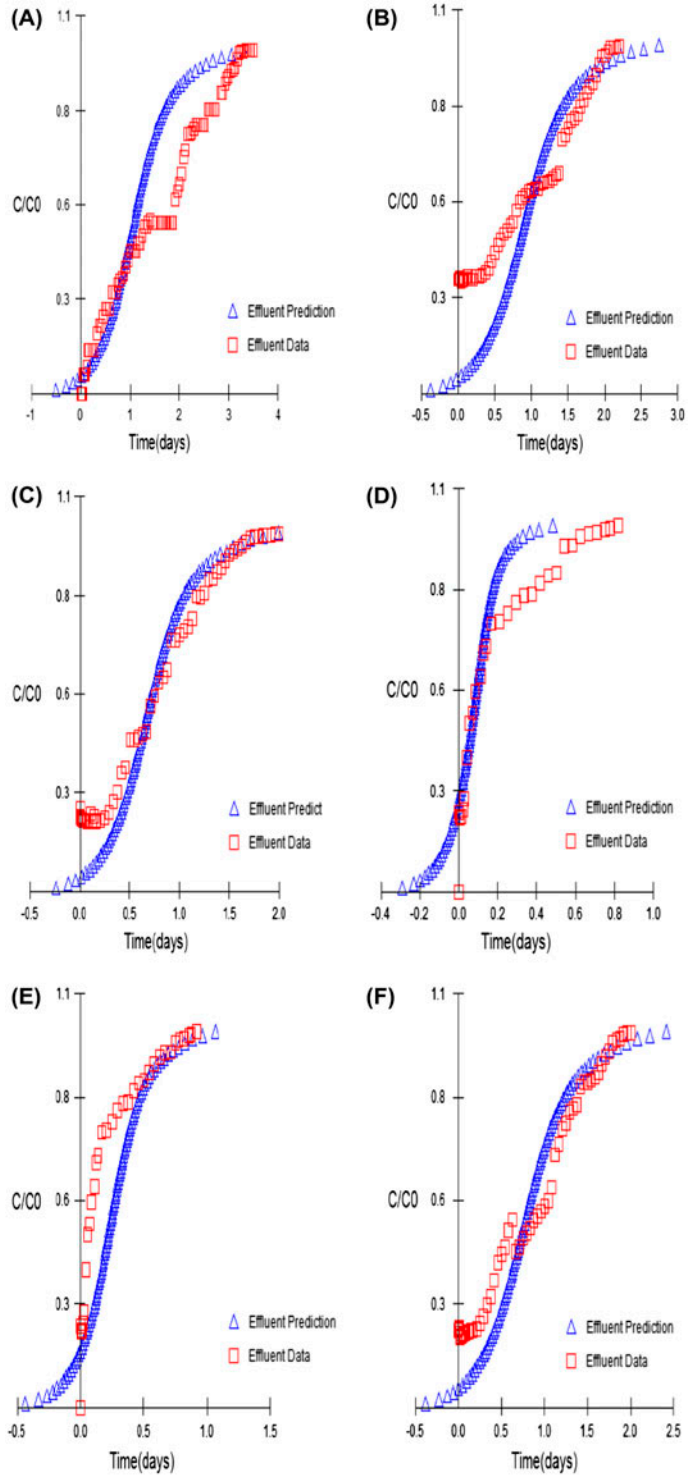

Fig. 7. CPHSDM plot of the adsorption of (A) 1 mg/L MB dye onto 2 g (14.5 cm) of HYCA adsorbent (Flow rate = 5 mL/min; temperature = 30˚C) (B) 10 mg/L MB dye onto 2 g (14.5 cm) of HYCA adsorbent (Flow rate = 5 mL/min; temperature = 30˚C) (C) 15 mg/L MB dye onto 2 g (14.5 cm) of HYCA adsorbent (Flow rate = 5 mL/min; temperature = 30˚C) (D) 15 mg/L MB dye onto *0.5 g (3.5 cm)* of HYCA adsorbent (Flow rate = 5 mL/min; temperature = 30˚C) (E) 15 mg/L MB dye onto *1.0 g (7.25 cm)* of HYCA adsorbent (Flow rate = 5 mL/min; temperature = 30˚C) (F) 15 mg/L MB dye onto *2.0 g* (14.5 cm) of HYCA adsorbent (Flow rate = 5 mL/min; *temperature* = 40˚C) (G) 15 mg/L MB dye onto 2 g (14.5 cm) of HYCA adsorbent (Flow rate = 5 mL/min; *temperature* = 50˚C) (H) 15 mg/L MB dye onto 2 g (14.5 cm) of HYCA adsorbent (Flow rate = 7.5 mL/min; temperature = 30˚C) (I) 15 mg/L MB dye onto 2 g (14.5 cm) of HYCA adsorbent (Flow rate = 10 mL/min; temperature = 30˚C).

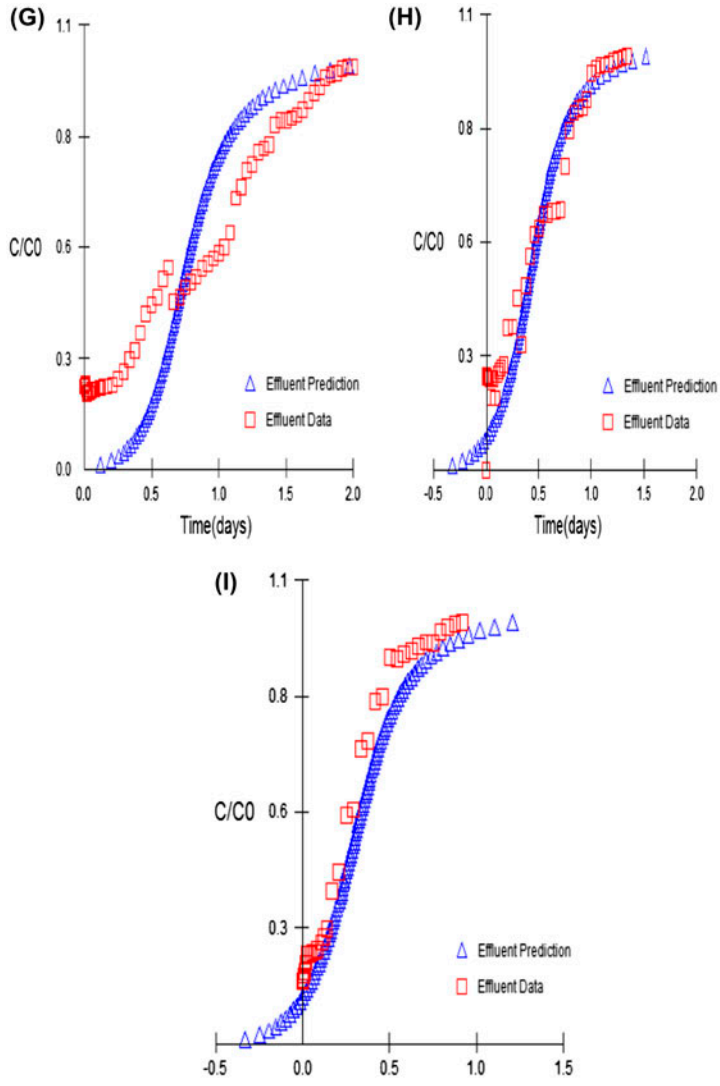

Fig. 7. (*Continued*).

In the presence of other organic pollutants with same treatment objective, the breakthrough volume capacity and breakthrough time of HYCA adsorbent were predicted to decrease to 1.3 m^3 (0.26 m^3 each cycle) and 8 h 58 min (1 h 43 min each run) using a Wausau Ground water model (a low organic fouling agent) as found in AdDesignS^{TM} as a reference. This is a 10% reduction in the efficiency of the HYCA adsorbent. Moreover, 1 kg of HYCA adsorbent will attain 95% breakthrough (95% of 1 mg/L MB dye being released into effluent solution) under similar operating conditions after ca. 2.11 d (50 h 38 min) and after treating 7.60 m^3 of contaminated water.

In summary, HYCA prepared from a composite of kaolinite clay and *C. papaya* seeds was used for the adsorption of MB in a fixed bed. Modeling experimental data with the Thomas model suggest that increasing initial dye concentration, bed height, and temperature increase the breakthrough adsorption capacity of HYCA for MB. On the contrary, increasing flow rate reduces the breakthrough adsorption. The PSDM describes experimental data better than the CPHSDM. With the PSDM, AdDesignS^{TM} software predicts that 1 kg HYCA will treat 1.45 m^3 (0.29 m^3 each cycle) of water containing 1 mg/L of MB with a treatment objective of 50 μg/L MB dye effluent solution in 9 h 35 min. The presence of other organic pollutants in low concentrations "fouling" the MB solution may reduce the adsorption capacity of HYCA by 10%. Desorption data showed that HYCA does not lose its efficiency at least in five regeneration cycles at temperatures below 50˚C with 0.01 M HNO_3.

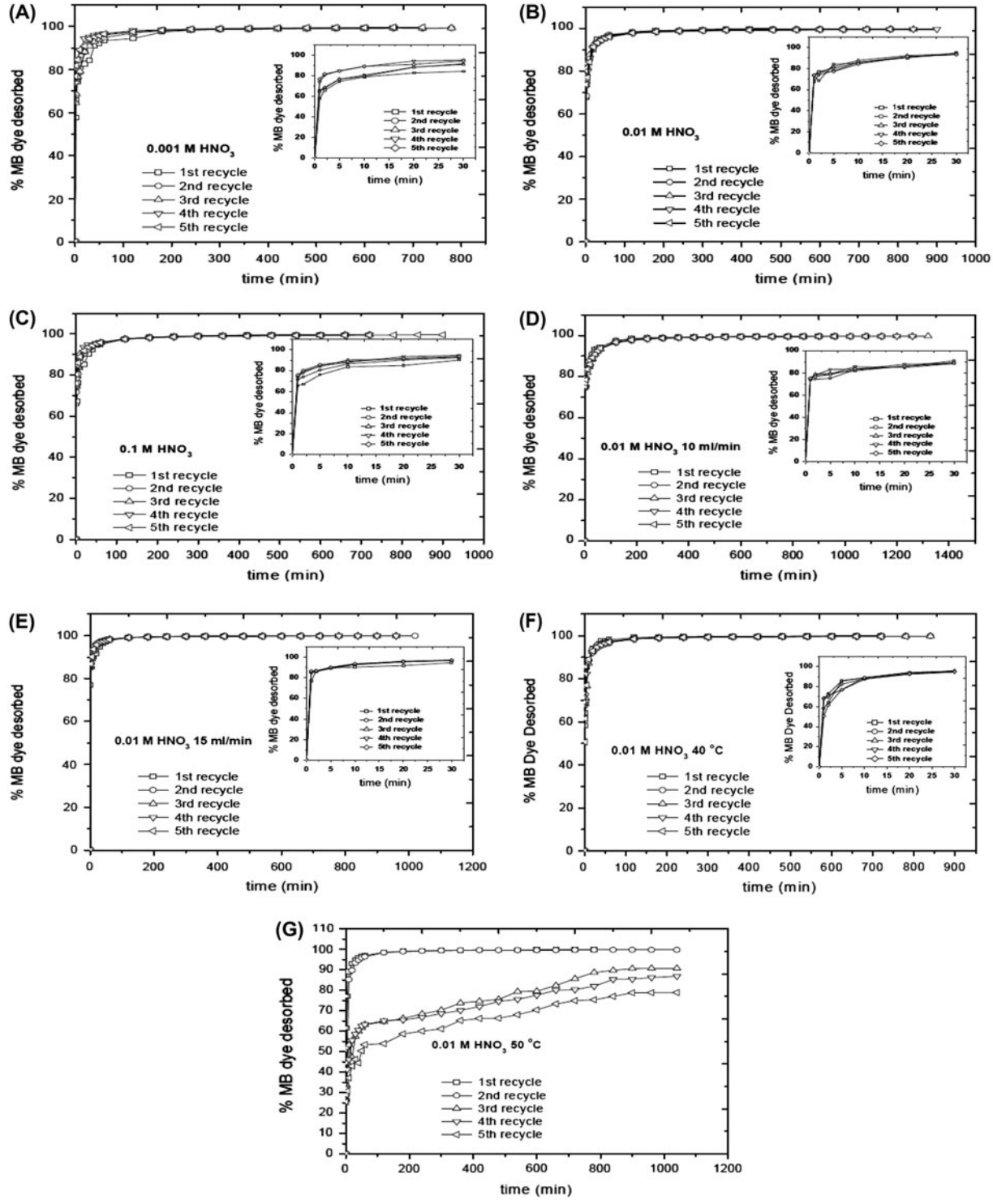

Fig. 8. Desorption plots of MB dye from HYCA adsorbent using (A) 0.001 M HNO_3 (flow rate = 5 mL/min; temperature = 30°C); (B) 0.01 M HNO_3 (flow rate = 5 mL/min; temperature = 30°C); (C) 0.1 M HNO_3 (flow rate = 5 mL/min; temperature = 30°C); (D) 0.01 M HNO_3 (flow rate = 10 mL/min; temperature = 30°C); (E) 0.01 M HNO_3 (flow rate = 15 mL/min; temperature = 30°C); (F) 0.01 M HNO_3 (flow rate = 5 mL/min; temperature = 40°C); (G) 0.001 M HNO_3 (flow rate = 5 mL/min; temperature = 50°C).

4. Conclusion

This and our previous study [8] provide a baseline data that are promising for up-scaling the adsorption of cationic organic pollutants from aqueous solution using a new hybrid adsorbent, HYCA. The use of HYCA instead of activated carbon and zeolites will definitely be economical in terms of its cost, availability, and efficiency.

Acknowledgments

The authors thank Dr Harji Bashir (Cambridge Reactor Design) for support with the Salamander Reactor. E.I.U. gratefully acknowledges a The World Academy of Sciences (TWAS)-United Nations Education, Science and Cultural Organization (UNESCO) Research Grant (RGA 10-215 RG/CHE/AF/AC_1-UNESCO FR: 3240245996). The authors also acknowledge support from the Redeemer's University, the University of Potsdam, and the Alexander von Humboldt Foundation enabling the intense collaboration between the partners.

References

[1] C.-H. Weng, Y.-T. Lin, T.-W. Tzeng, Removal of methylene blue from aqueous solution by adsorption onto pineapple leaf powder, J. Hazard. Mater. 170 (2009) 417–424.
[2] A. Gottlieb, C. Shaw, A. Smith, A. Wheatley, S. Forsythe, The toxicity of textile reactive azo dyes after hydrolysis and decolourisation, J. Biotechnol. 101 (2003) 49–56.
[3] B. Yasemi, A. Haluk, A kinetics and thermodynamics study of methylene blue adsorption on wheat shells, Desalination 194 (2006) 259–267.
[4] V.K. Gupta, S. Agarwal, P. Singh, D. Pathania, Acrylic acid grafted cellulosic Luffa cylindrical fiber for the removal of dye and metal ions, Carbohydr. Polym. 98 (2013) 1214–1221.
[5] J. Zhang, Q. Ping, M. Niu, H. Shi, N. Li, Kinetics and equilibrium studies from the methylene blue adsorption on diatomite treated with sodium hydroxide, Appl. Clay Sci. 83–84 (2013) 12–16.
[6] E.I. Unuabonah, M.I. El-Khaiary, B.I. Olu-owolabi, K.O. Adebowale, Predicting the dynamics and performance of a polymer-clay based composite in a fixed bed system for the removal of lead (II) ion, Chem. Eng. Res. Des. 90 (2012) 1105–1115.
[7] R.R. Gonte, G. Shelar, K. Balasubramanian, Polymer–agro-waste composites for removal of congo red dye from wastewater: Adsorption isotherms and kinetics, Desalin. Water Treat. (2013), doi: 10.1080/19443994.2013.833876.
[8] B.H. Hameed, A.A. Ahmad, Batch adsorption of methylene blue from aqueous solution by garlic peel, an agricultural waste biomass, J. Hazard. Mater. 164 (2009) 870–875.
[9] A.A. Ahmad, A. Idris, B.H. Hameed, Organic dye adsorption on activated carbon derived from solid waste, Desalin. Water Treat. 51 (2013) 2554–2563.
[10] E.I. Unuabonah, G.U. Adie, L.O. Onah, O.G. Adeyemi, Multistage optimization of the adsorption of methylene blue dye onto defatted *Carica papaya* seeds, Chem. Eng. J. 155 (2009) 567–579.
[11] E.I. Unuabonah, C. Gunter, J. Weber, S. Lubahn, A. Taubert, Hybrid clay: A new highly efficient adsorbent for water treatment, ACS Sustain. Chem. Eng. 1 (2013) 966–973.
[12] K.O. Adebowale, I.E. Unuabonah, B.I. Olu-owolabi, Adsorption of some heavy metal ions on sulfate- and phosphate-modified kaolin, Appl. Clay Sci. 29 (2005) 145–148.
[13] S.H. Lin, R.S. Juang, Y.H. Wang, Adsorption of acid dye from water onto pristine and acid-activated clays in fixed beds, J. Hazard. Mater. 113 (2004) 195–200.
[14] P. Suksabye, P. Thiravetyan, W. Nakbanpote, Column study of chromium(VI) adsorption from electroplating industry by coconut coir pith, J. Hazard. Mater. 160 (2008) 56–62.
[15] H.C. Thomas, Heterogeneous ion exchange in a flowing system, J. Am. Chem. Soc. 66 (1944) 1664–1666.
[16] G.S. Bohart, E.Q. Adams, Some aspects of the behavior of charcoal with respect to chlorine, J. Am. Chem. Soc. 42 (1920) 523–544.
[17] R.M. Clark, Evaluating the cost and performance of field-scale granular activated carbon systems, Environ. Sci. Technol. 21 (1987) 573–580.
[18] Y.H. Yoon, J.H. Nelson, Application of gas adsorption kinetics I. A theoretical model for respirator cartridge service life, Am. Ind. Hyg. Assoc. J. 45 (1984) 509–516.
[19] D.W. Hand, J.C. Crittenden, W.E. Thacker, Simplified models for design of fixed-bed adsorption systems, J. Environ. Eng. 110 (1984) 440–456.
[20] D.C.K. Ko, J.F. Porter, G. McKay, Film-pore diffusion model for the fixed-bed sorption of copper and cadmium ions onto bone char, Water Res. 35 (2001) 3876–3886.
[21] E. Worch, Modelling the solute transport under non-equilibrium conditions on the basis of mass transfer equations, J. Contam. Hydro. 68 (2004) 97–120.
[22] J.C. Crittenden, N.J. Hutzler, D.G. Geyer, J.L. Oravitz, G. Friedman, Transport of organic compounds with saturated groundwater flow: Model development and parameter sensitivity, Water Resour. Res. 22 (1986) 271–284.
[23] Z. Ma, R.D. Whitley, N.-H.L. Wang, Pore and surface diffusion in multicomponent adsorption and liquid chromatography systems, AlChE J. 42 (1996) 1244–1262.
[24] B.A. Finlayson, The Method of Weighted Residuals and Variational Principles, Academic Press, New York, NY, 1972.
[25] B.A. Finlayson, Non Linear Analysis in Chemical Engineering, McGraw-Hill, New York, NY, 1980.
[26] J. Villadsen, M.L. Michelsen, Solution of Differential Equation Models by Polynomial Approximation, Prentice-Hall, Englewood Cliffs, NJ, 1978.
[27] G. Friedman, Mathematical Modeling of Multicomponent Adsorption in Batch and Fixed-Bed Reactors, Michigan Technological University, Houghton, MI, 1984.

[28] Z. Aksu, F. Gönen, Biosorption of phenol by immobilized activated sludge in a continuous packed bed: Prediction of breakthrough curves, Process Biochem. 39 (2004) 599–613.
[29] T.V.N. Padmesh, K. Vijayaraghavan, G. Sekaran, M. Velan, Batch and column studies on biosorption of acid dyes on fresh water macro alga *Azolla filiculoides*, J. Hazard. Mater. 125 (2005) 121–129.
[30] R. Han, Y. Wang, W. Yu, W. Zou, J. Shi, H. Liu, Biosorption of methylene blue from aqueous solution by rice husk in a fixed-bed column, J. Hazard. Mater. 141 (2007) 713–718.
[31] F. Banat, S. Al-Asheh, R. Al-Ahmad, F. Bni-Khalid, Bench-scale and packed bed sorption of methylene blue using treated olive pomace and charcoal, Bioresour. Technol. 98 (2007) 3017–3025.
[32] R. Han, Y. Wang, W. Zou, Y. Wang, J. Shi, Comparison of linear and nonlinear analysis in estimating the Thomas model parameters for methylene blue adsorption onto natural zeolite in fixed-bed column, J. Hazard. Mater. 145 (2007) 331–335.
[33] V.C. Taty Costodes, H. Fauduet, C. Porte, Y.-S. Ho, Removal of lead (II) ions from synthetic and real effluents using immobilized *Pinus sylvestris* sawdust: Adsorption on a fixed-bed column, J. Hazard. Mater. 123 (2005) 135–144.
[34] T.S. Singh, K.K. Pant, Experimental and modelling studies on fixed bed adsorption of As (III) ions from aqueous solution, Sep. Purif. Technol. 48 (2006) 288–296.
[35] S. Kundu, A.K. Gupta, As(III) removal from aqueous medium in fixed bed using iron oxide-coated cement (IOCC): Experimental and modeling studies, Chem. Eng. J. 129 (2007) 123–131.
[36] S. Ghorai, K.K. Pant, Investigations on the column performance of fluoride adsorption by activated alumina in a fixed bed, Chem. Eng. J. 98 (2004) 165–173.
[37] K. Vijayaraghavan, J. Jegan, K. Palanivelu, M. Velan, Removal of nickel (II) ions from aqueous solution using crab shell particles in a packed bed up-flow column, J. Hazard. Mater. 113 (2004) 223–230.
[38] A. Pallavi, Made in India, 2011, February 28. Available from http://www.downtoearth.org.in/content/made-india.